Journal of Power Sources 201 (2012) 301–306

Contents lists available at SciVerse ScienceDirect

Journal of Power Sources

journal homepage: www.elsevier.com/locate/jpowsour

Synthesis of $Li_3V_2(PO_4)_3$ cathode material via a fast sol–gel method based on spontaneous chemical reactions

Wei Yuan[a,*], Ji Yan[a], Zhiyuan Tang[a], Ou Sha[a], Jinmei Wang[a], Wenfeng Mao[a], Li Ma[b]

[a] Department of Applied Chemistry, School of Chemical Engineering and Technology, Tianjin University, Tianjin 300072, China
[b] McNair Technology Co., Ltd., Dongguan, Guangdong 523700, China

ARTICLE INFO

Article history:
Received 25 September 2011
Received in revised form 1 November 2011
Accepted 17 November 2011
Available online 25 November 2011

Keywords:
Lithium ion batteries
Lithium vanadium phosphate
Fast sol–gel
High rate
Spontaneous chemical reaction

ABSTRACT

A fast sol–gel method based on spontaneous chemical reactions is developed to synthesize high performance $Li_3V_2(PO_4)_3$/C cathode material. The crystal structures, surface morphologies and electrochemical behaviors of the $Li_3V_2(PO_4)_3$/C samples sintered at different temperatures are investigated. In the potential range of 3.0–4.3 V, the sample sintered at 750 °C shows the highest discharge capacities of 127.9 mAh g^{-1} and 124.0 mAh g^{-1} at 1*C* and 5*C* rates after 100 cycles respectively. Furthermore, at 10*C*, 15*C* and 20*C* rates, the discharge capacities of the optimal $Li_3V_2(PO_4)_3$/C composite still retains 117.6 mAh g^{-1}, 114.9 mAh g^{-1} and 83.6 mAh g^{-1} in the 150th cycle respectively. Cyclic voltammetry (CV) measurement illustrates that the electrochemical behavior of the optimal sample almost has no change after 100 cycles at 5*C* rate, indicating the stable structure of the synthesized material.

1. Introduction

In past decades, lithium ion batteries have been rapidly developed as a portable energy storage device. Compared with nickel–cadmium and nickel–hydrogen secondary batteries, lithium ion batteries have high energy density, low self-discharge ratio, and long calendar life. Layered $LiCoO_2$ [1] was first used as cathode material in commercial lithium ion batteries, but due to its disadvantages of high cost, toxicity and low rate-capability, various candidates for $LiCoO_2$ have been investigated continually. Especially, $LiNiO_2$, $LiMnO_2$ and $LiMn_2O_4$ have attracted intensive attention of worldwide researchers for their extraction/insertion property of lithium ions [2–4], but some insuperable drawbacks existed in these cathode materials still limit their practical application [5]. In 1997, Goodenough et al. [6] first reported a series of NASICON (Sodium Silicon Ionic Conductor) structural cathode materials based on phosphate, such as $Li_2NaV_2(PO_4)_3$, $LiNa_2FeV(PO_4)_3$, $TiNb(PO_4)_3$, $LiFeNb(PO_4)_3$, and $Li_2FeTi(PO_4)_3$. However, as a derivative of $Li_2NaV_2(PO_4)_3$, $Li_3V_2(PO_4)_3$ reported firstly by Nazar et al. [7–9] is considered as one of the most promising candidates for commercial cathode materials.

$Li_3V_2(PO_4)_3$ (LVP) has the highest theoretic capacity (197 mAh g^{-1}) among all phosphate cathode materials when three lithium ions are extracted from the NASICON structure. Moreover, the unique NASICON structure provides a 3D framework and a large interstitial space for lithium ions transfer [7]. Tang et al. [10] and Qiao et al. [11] disclosed that the lithium ion diffusion coefficient of $Li_3V_2(PO_4)_3$ varies from 10^{-8} to 10^{-9} cm^2 s^{-1}, which is much higher than that of $LiFePO_4$ [12]. On the other hand, phosphate plays a key role in stabilizing the whole crystal structure and endows $Li_3V_2(PO_4)_3$ a good stability even at a high potential. However, the electronic conductivity of pristine $Li_3V_2(PO_4)_3$ only reaches 10^{-7} S cm^{-1} [9] that is much lower than that of $LiCoO_2$ at room temperature [13]. In recent years, tremendous efforts have been made to overcome this defect, such as through carbon and metal oxides coating [14–18], cation and anion doping [19–22]. Hereinto, the carbon coating is the most effective way to enhance the electronic conductivity of $Li_3V_2(PO_4)_3$ that can achieve 10^{-1} S cm^{-1}[14]. Whereas, after coating the carbon layer on the surface of $Li_3V_2(PO_4)_3$ particles, the tap density of the material will be decreased, as well as the energy density. In previous literatures [16,23], the reported carbon contents of $Li_3V_2(PO_4)_3$/C were more than 10% in weight. Hence, it is necessary to prepare the low carbon content $Li_3V_2(PO_4)_3$/C cathode material with excellent electrochemical performances.

It is well known that solid state reaction, microwave irradiation, and sol–gel methods are the main routes to synthesize the $Li_3V_2(PO_4)_3$/C cathode material [24–27]. However, the solid state reaction method needs high sintering temperature and long sintering time that leads to a wide range of particle size distribution, resulting in poor rate capability and hampering its practical application in lithium ion batteries. As a fast route to synthesize

* Corresponding author. Tel.: +86 83017180, fax: +86 0769 83195372.
E-mail address: yuanwei.390@163.com (W. Yuan).

0378-7753/$ – see front matter © 2011 Elsevier B.V. All rights reserved.
doi:10.1016/j.jpowsour.2011.11.051

$Li_3V_2(PO_4)_3$/C, the microwave method possesses an advantage of low energy consumption, but it is difficult to mass production. The sol–gel method can promote raw materials to reach atomic level mixing and homogenously trap inside the interconnected viscous gel, which reduces particle size of the material to micrometer or nanometer level. In addition, the sintering temperature and time can be lowered significantly. But the complex synthesizing process makes it difficult implement in practical production.

In the present work, we introduce a fast sol–gel method based on spontaneous chemical reactions among raw materials to prepare $Li_3V_2(PO_4)_3$/C. It not only possesses the advantages of the traditional sol–gel method, but also has a simple synthesis process that has a potential to mass production under low energy consumption. What is more, the prepared material with low carbon content exhibits outstanding electrochemical performances, especially in high rate and long term cyclic properties. It should be noted that all the capacities in the paper are calculated from the $Li_3V_2(PO_4)_3$ weight.

2. Experimental

The $Li_3V_2(PO_4)_3$/C cathode materials were prepared through the fast sol–gel method. 0.015 mol Li_2CO_3, 0.01 mol V_2O_5 and 0.03 mol $NH_4H_2PO_4$ were mixed in 2.0 mL deionized water coupled with spontaneous endothermic reaction under continuous stirring, and a mass of gas was produced in this process. Citric acid employed as both chelating reagent and carbon source was dissolved in 8.0 mL deionized water, and the amount of citric acid was based on the residual carbon content of $Li_3V_2(PO_4)_3$/C. Then the citric acid solution was blended with the above mixture under continuous stirring until the mixture turned to clear sol. Excess water was evaporated at 80 °C in a water bath until a dark blue gel was obtained. The dry gel was carefully grinded for 1 h, and presintered at 350 °C for 4 h under a flowing high pure N_2 to release H_2O, CO_2, and NH_3. Then the precursor was pressed to pellets at 15 MPa, and heated at different temperatures from 700 °C to 800 °C for 8 h under the gas flow of high pure N_2 to yield $Li_3V_2(PO_4)_3$/C.

The crystal structures of the $Li_3V_2(PO_4)_3$/C samples were characterized employing a PTR III X-ray diffractometer (XRD) with Cu Kα radiation. The morphologies of the as-prepared materials were observed using JSM-6380LA scanning electron microscope (SEM) and high-resolution transmission electron microscopy (TEM, tecnai G2 F20).

The electrochemical performances of the synthesized $Li_3V_2(PO_4)_3$/C materials were studied employing 2032 coin-type cells. Cathode electrodes were prepared by mixing 80 wt.% the as-synthesized $Li_3V_2(PO_4)_3$/C materials with 10 wt.% acetylene black and 10 wt.% polytetrafluoroethylene (PTFE, 60 wt.%). Metallic lithium foil was employed as the anode. The electrolyte was 1 M $LiPF_6$ in ethylene carbonate (EC) and dimethyl carbonate (DMC) (1:1 in volume), and the separator was Celgard 2300. The coin cells were assembled in an argon filled glove box, and then charge/discharge tests were operated on a LISUN-CBT-138-32 multichannel battery test system in the voltage range of 3.0–4.3 V (vs. Li/Li^+). Cyclic voltammetry (CV) tests were conducted on a GAMRY PC14-750 electrochemical workstation at a scanning rate of 0.1 mV s^{-1} in the voltage range of 3.0–4.4 V.

3. Results and discussion

3.1. Synthesis of the $Li_3V_2(PO_4)_3$/C precursor

The whole process of synthesizing the $Li_3V_2(PO_4)_3$/C precursor can be divided into two stages. The first stage is to mix the raw materials with 2.0 mL deionized water. As above mentioned, this process is a spontaneous endothermic reaction. Water plays a significant role as initiator inducing $NH_4H_2PO_4$ to dissociate, and the dissociated H^+ causes Li_2CO_3 to decompose into CO_2 and H_2O. With the consumption of H^+ and the generation of H_2O, the dissociation of $NH_4H_2PO_4$ is intensified increasingly, so this process is stimulated like a chain reaction. Furthermore, the decomposition product CO_2 also acts as a dispersant that promotes the raw material to form a uniform wet gel.

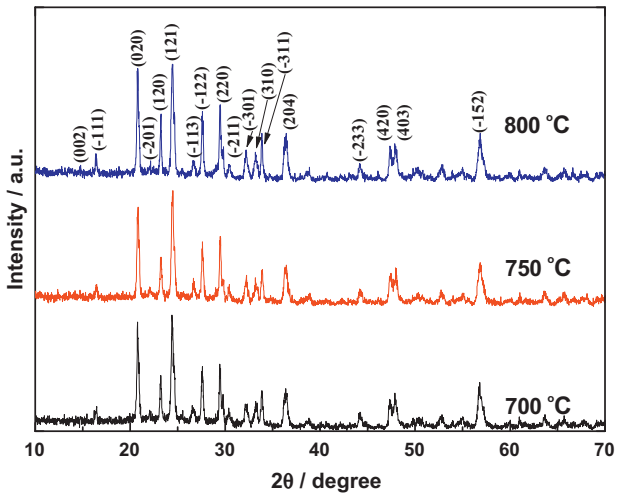

Fig. 1. XRD patterns of the $Li_3V_2(PO_4)_3$/C samples synthesized at different temperatures.

The second stage is a cheating process by adding citric acid into the above wet gel under continuous stirring, the mixture rapidly changes to a clear red brown sol in company with the release of heat generated from complexation. During heating in water bath, the color of the sol turns to dark blue, indicating that pentavalent vanadium has been reduced to quadrivalent vanadium by citric acid [28]. This may be the reason that the low sintering temperature can be obtained in this method. In addition, the oxidized product CO_2 from citric acid promotes raw materials to further mix in atomic level, which is a key to synthesize the excellent electrochemical performance material.

3.2. Characterization of $Li_3V_2(PO_4)_3$/C samples

The XRD patterns of the prepared $Li_3V_2(PO_4)_3$/C at different sintering temperatures are shown in Fig. 1. In all cases, the synthesized $Li_3V_2(PO_4)_3$/C are found to have the same monoclinic structure with space group $P2_1/n$, and no impurity phases such as Li_3PO_4, Li_2O and V_2O_3 are detected, indicating that the pure $Li_3V_2(PO_4)_3$/C cathode material can be obtained in the temperature range of 700–800 °C. What is more, no signs of the coating carbon are found, because of its low content or amorphous structure. Meanwhile, it demonstrates that the coating carbon does not influence the structure of the as-prepared materials. The residual carbon contents of $Li_3V_2(PO_4)_3$/C that were calculated by referring the literature [16] are 4.56%, 3.34% and 1.57% at 700 °C, 750 °C and 800 °C, respectively. The residual carbon contents decrease with the sintering temperature increasing, which is in good agreement with the previous report [16].

The morphologies of the samples sintered at 700 °C, 750 °C and 800 °C are shown in Fig. 2(a)–(c). It can be clearly observed that all the samples have loose porous morphology, and the particle sizes reach to sub-micrometer level, although the shape of particles is irregular. It is noted that this microstructure has a large specific surface area allowing the electrolyte to keep adequate contact with the active material, which may be beneficial for the high rate

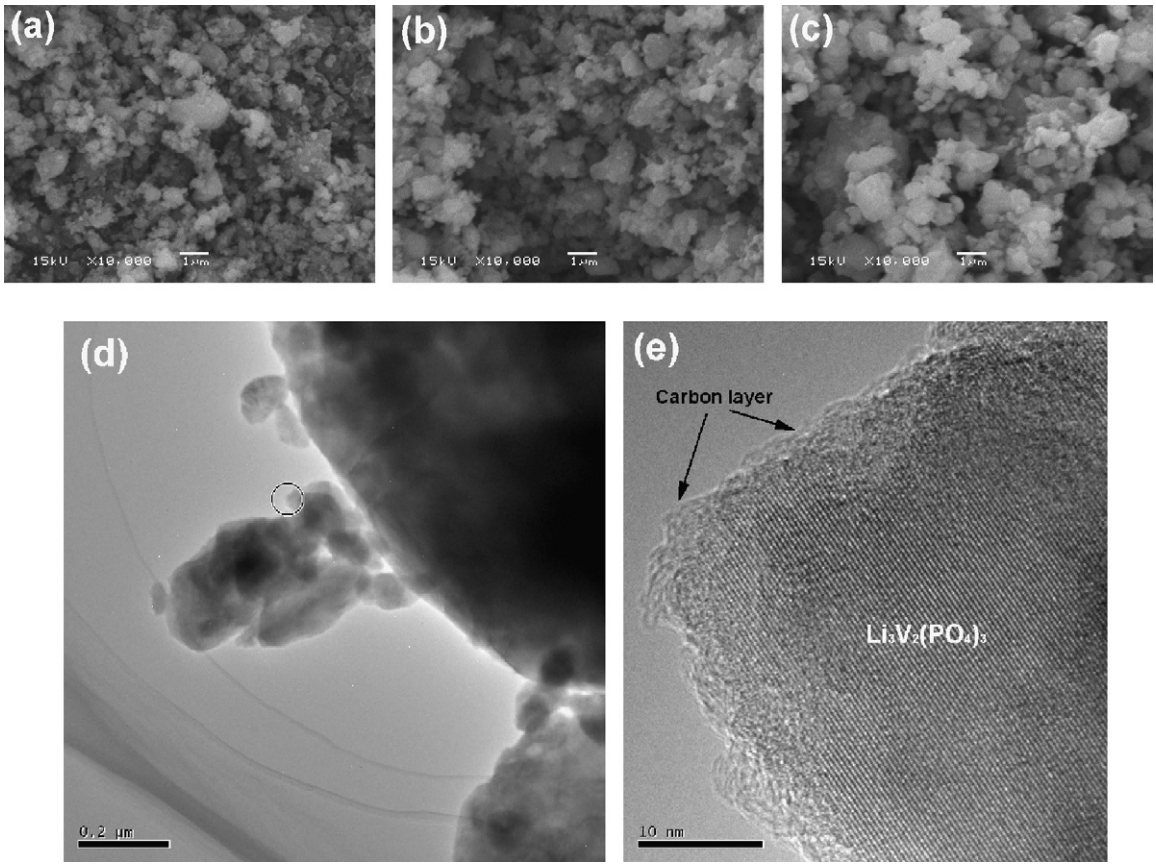

Fig. 2. SEM images of the $Li_3V_2(PO_4)_3$ samples synthesized at (a) 700 °C, (b) 750 °C, and (c) 800 °C, (d) TEM and (e) HRTEM images of the $Li_3V_2(PO_4)_3$/C sample synthesized at 750 °C.

performance. Considering the preparation process of the precursor, we conclude that the formation of the loose porous microstructure is mainly attributed to the continuous production of the huge amounts of gas. In addition, the sample sintered at 700 °C has the smallest particle size, but the loose porous degree is not as high as the samples sintered at 750 °C and 800 °C. However, palpable agglomeration occurs when the temperature increases to 800 °C. In contrast, the sample sintered at 750 °C not only has a small particle size, but also has a uniform morphology with loose porous microstructure. In order to prove the existence of the carbon layer on the surface of $Li_3V_2(PO_4)_3$/C particles, TEM analysis was carried out. As shown in Fig. 2(d) and (e), a thin carbon layer, about 2–3 nm, is coated on particle surface, and the thin carbon layer is consistent with the low amount of residual carbon in the $Li_3V_2(PO_4)_3$/C composite. Interestingly, the relatively uniform amorphous carbon layer is still formed even under the condition of the continuous gas production, and the formed carbon shell is believed to prevent the crystal growth of $Li_3V_2(PO_4)_3$/C, which plays a significant role in enhancing the electrochemical performances. The lattice planes of $Li_3V_2(PO_4)_3$/C are distinct as shown in Fig. 2(e), meaning a high crystallinity of $Li_3V_2(PO_4)_3$/C sintered at 750 °C.

3.3. Electrochemical performances

Fig. 3(a) and (b) shows the charge and discharge curves of three samples at 1*C* rate (1*C* = 133 mA g^{-1}) and 5*C* rate in the potential range of 3.0–4.3 V at room temperature. All the curves show a similar shape presenting three charge/discharge plateaus that correspond to three kinds of reversible phase transformation between $Li_{3-x}V_2(PO_4)_3$ (x = 0, 0.5, 1.0, and 2.0). As shown in the profiles, the sample sintered at 750 °C delivers the highest discharge capacities of 128.8 mAh g^{-1} and 124.1 mAh g^{-1} achieving 96.8% and 93.3% of its theoretical capacity (133 mAh g^{-1}) at 1*C* and 5*C* rates respectively, as compared to 115.7 mAh g^{-1} and 123.8 mAh g^{-1} at 1*C* rate, 103.0 mAh g^{-1} and 110.9 mAh g^{-1} at 5*C* rate of the samples synthesized at 700 °C and 800 °C, respectively. What is more, we find that the sample sintered at 750 °C has the lowest plateaus voltage separations, and we ascribe this to the lowest electrochemical polarization and the best reversibility of the optimal sample.

The cyclic performance of three samples at 1*C* and 5*C* rates for 100 cycles are presented in Fig. 3(c) and (d) respectively. As shown in the profiles, the sample sintered at 750 °C has the highest discharge capacities of 127.9 mAh g^{-1} and 124.6 mAh g^{-1} after 100 cycles at 1*C* and 5*C* rates respectively, these results are much higher than that of the previous reports [14,15,17]. The other two samples sintered at 700 °C and 800 °C deliver the discharge capacities of 117.7 mAh g^{-1} and 122.6 mAh g^{-1} at 1*C* rate, 105.2 mAh g^{-1} and 110.1 mAh g^{-1} at 5*C* rate in the 100th cycle respectively. It should be mentioned that the capacities of the materials have an increasing process at the initial cycles, and then become stable after several cycles. This phenomenon is mainly attributed to a continuous increasing active surface area of the material resulting from the gradual penetration of the electrolyte into particle interspace [29]. Moreover, the discharge capacities of all the samples decrease regularly compared with that of 1*C* rate when the charge/discharge current density increases to 5*C* rate, this may be caused by electrochemical polarization in high current density. Even undergoing 100 cycles test, the discharge capacities of three samples do not tend to fade both at 1*C* and 5*C* rates, although the ones sintered at 700 °C and 800 °C exhibit lower capacities. This excellent cyclic performance may be attributed to the intrinsic stability of NASICON framework [7]. However, low sintering temperature may induce a

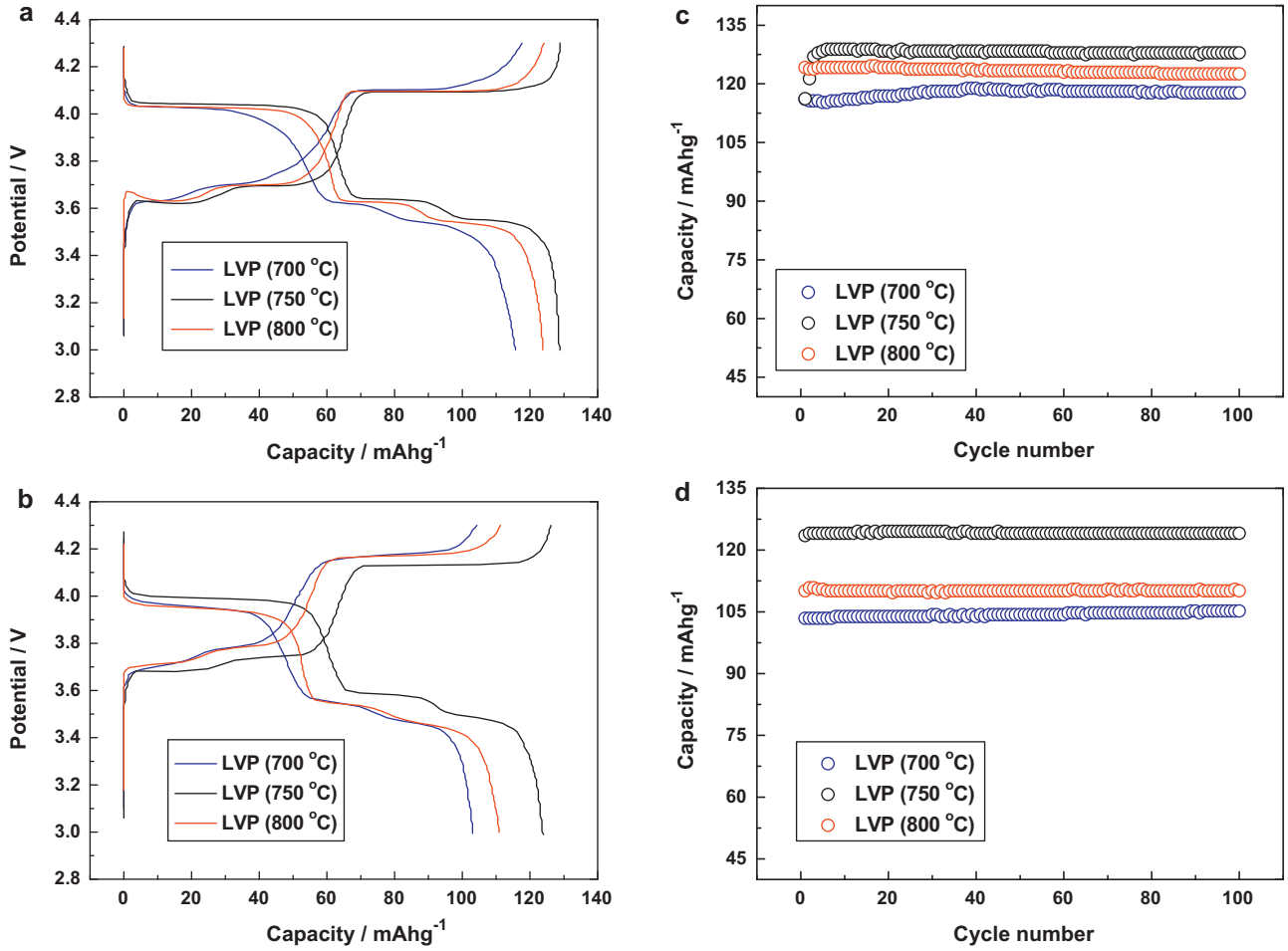

Fig. 3. Charge and discharge curves at (a) 1*C* rate and (b) 5*C* rate, and cyclic performance at (c) 1*C* rate and (d) 5*C* rate of the $Li_3V_2(PO_4)_3$/C samples synthesized at different temperatures.

lower crystallinity of the material that is not beneficial for high electrochemical performance. High sintering temperature leads small primary particles to form large agglomerated particles that prolong the diffusion path of lithium ions as shown in Fig. 2(c), which is adverse for improving electrochemical performance. On the other hand, the thick carbon layer of the sample sintered at 700 °C may block the path of lithium ions from electrode to electrolyte, and the lower carbon content of the sample sintered at 800 °C does not favor the enhancement of the electron conductivity [16].

It is well known that the high rate capability is an important factor to influence application for lithium ion batteries in electric vehicles and mobile devices. Whereas, to further investigate the high rate performance of the sample sintered at 750 °C, we increased the charge/discharge current density to 10*C*, 15*C* and 20*C*. The results are shown in Fig. 4. We can see that the sample reaches the peak discharge capacities of 121.8 mAh g^{-1} in the 6th cycle at 10*C* rate, 121.8 mAh g^{-1} in the 20th cycle at 15*C* rate and 120.0 mAh g^{-1} in the 1st cycle at 20*C* rate. The discharge capacities still retains 117.6 mAh g^{-1}, 114.9 mAh g^{-1} and 83.6 mAh g^{-1} after 150 cycles at 10*C*, 15*C* and 20*C* rates respectively. These results are much better than that of the reported results [23,30–32]. It is worth notice that the long term cyclic capability at 20*C* rate has never been reported yet, although the capacity of the sample fades sharply after 110 cycles, they keep at satisfactory values. We consider that the coating carbon in situ formed via the pyrolysis of citric acid on the surface of $Li_3V_2(PO_4)_3$ and the loose porous microstructure contribute mostly to this excellent high rate property. First, the coating carbon modifies the surface potential of the material, and provides different lithium ion adsorption sites in a wide range of energies that is favor for lithium ions transfer between electrode and electrolyte [33]. Second, the depressed growth of the active material particle due to the coating carbon [34], together with the loose porous microstructure, which are beneficial for the electrolyte penetration and lithium ions diffusion. Third, the formed carbon network bridges the $Li_3V_2(PO_4)_3$ particles to boost the electron conductivity of the synthesized material largely [7]. Fourth, the carbon layer on the surface of the $Li_3V_2(PO_4)_3$ composite protects the metal ions from dissolving into the electrolyte, which maintains the stable structure of the material, and the fracture of the material will also be restricted during cycling [21].

The insets of Fig. 4 show the charge and discharge curves of the sample at various cycles under 10*C*, 15*C* and 20*C* rates. It is apparent that the polarizations of the electrodes increase and the capacities decrease during the cyclic process. The decomposition of the electrolyte and the deterioration of the material structure during lithium ions extraction/insertion may take responsibility for this decay behavior. Additionally, we find that the position and the increasing rate of the third charge plateaus are crucial for high rate cyclic performance. As can be seen from Table 1, the third charge plateaus voltage increases with the charge rate increasing. However, the increasing rate of the third charge plateaus voltage at 20*C* rate is much higher than that of the electrode at 10*C* rate, and it is almost equal to that of the electrode at 15*C* rate. But the lower initial position of the third plateaus at 15*C* rate endows the

Table 1
The third charge plateaus voltages at various charge/discharge rates.

Charge/discharge rates (C)	Plateaus voltages of 25th cycle (V)	Plateaus voltages of 75th cycle (V)	Plateaus voltages of 150th cycle (V)
10	4.195	4.206	4.218
15	4.211	4.236	4.258
20	4.256	4.280	4.300

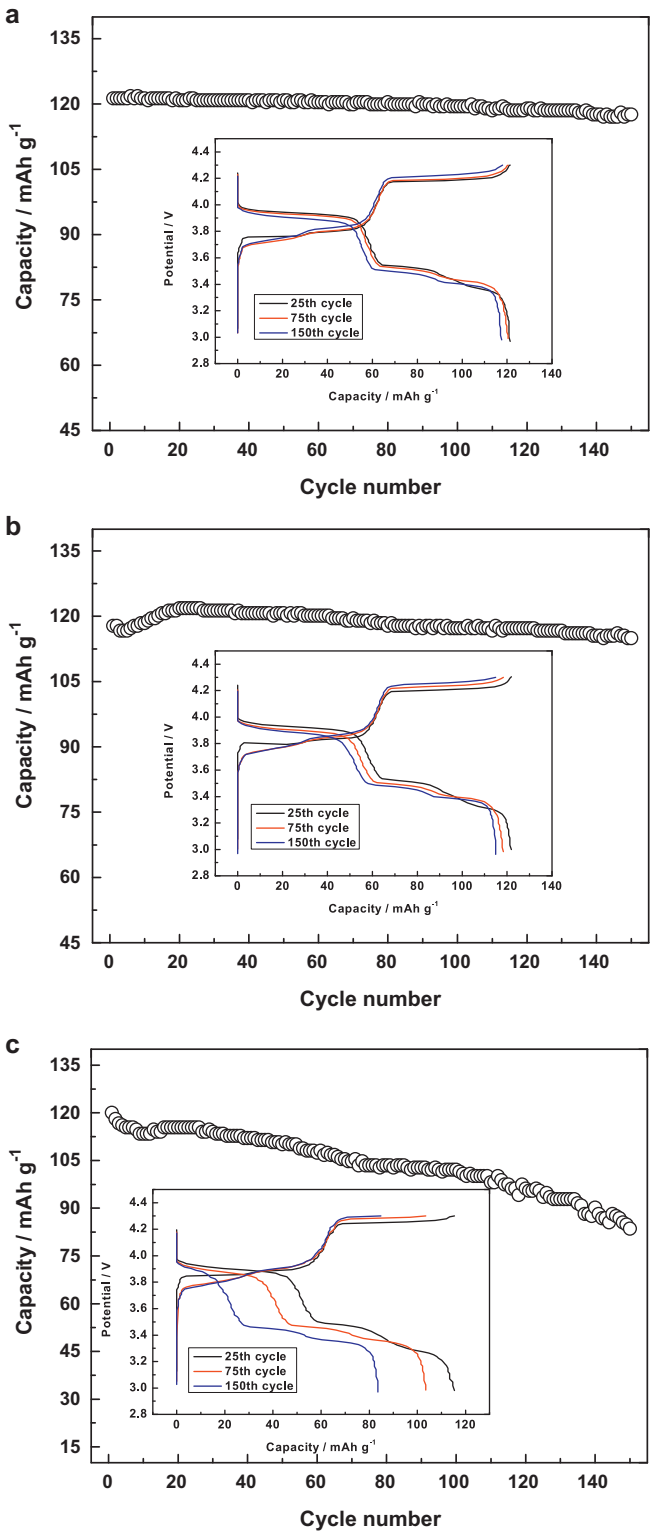

Fig. 4. Cyclic performance of the $Li_3V_2(PO_4)_3$/C sample synthesized at 750 °C (a) 10*C* rate, (b) 15*C* rate, (c) 20*C* rate. Insets are the 25th, 75th and 150th charge and discharge curves.

electrode an enough buffer space in a long term cycle, the higher initial position of the third charge plateaus at 20*C* rate make it easily reach the charge voltage limit (4.3 V). It can be observed that the third charge plateaus voltage has already been 4.3 V in the 150th cycle and the plateaus does not completely appear as shown in the inset of Fig. 4(c). Hence, decreasing the polarization, especially that of the third charge plateaus, is a key in order to further enhance the rate capability of $Li_3V_2(PO_4)_3$/C. If the charge mode is changed to a constant current plus constant voltage charge mode [35] or the charge voltage limit is increased slightly, the discharge capacity of the material may be enhanced greatly at high rate.

3.4. Cyclic voltammetry

To further investigate the electrochemical behaviors of the sample sintered at 750 °C, the CV curves of the electrode that were performed at a scan rate of 0.1 mV s^{-1} between 3.0 and s4.4 V at different states are shown in Fig. 5. Obviously, there are three sharp and symmetrical redox peaks in both curves representing the reversible extraction/insertion behavior of the first two lithium ions involving V^{3+}/V^{4+} redox couple, which are in good agreement with three charge/discharge plateaus in Fig. 3(a). As shown in Fig. 5, the electrode cycled at 0.5*C* rate for 10 cycles exhibits a good reversibility, and three oxidation peaks appear at 3.62 V, 3.70 V and 4.12 V, coupled with three reduction peaks at 3.55 V, 3.63 V and 4.02 V, respectively. But after the electrode has been cycled at 5*C* rate for another 100 cycles, we observe that all three oxidation peaks shift to higher potentials at 3.63 V, 3.71 V and 4.14 V respectively, the corresponding reduction peaks shift to lower potentials at 3.53 V, 3.62 V and 3.99 V respectively, indicating the reversibility of the electrode has been reduced slightly. However, the small potential separations between the cathodic peaks and the corresponding anodic peaks are still obtained, which illustrates the splendid structural stability of the synthesized material.

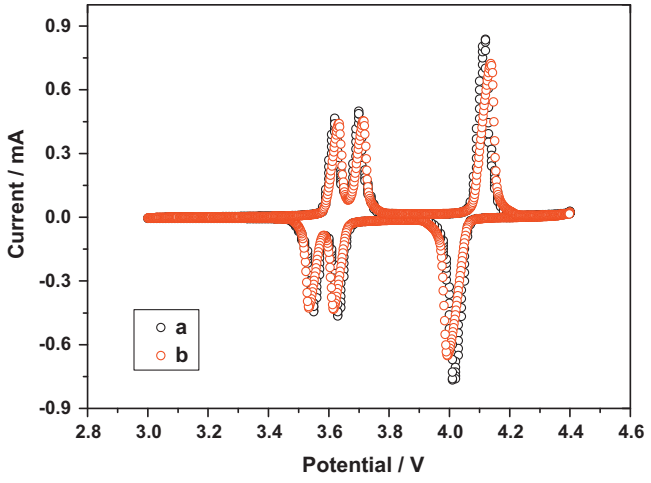

Fig. 5. CV curves (a) after 10 cycles at 0.5*C* rate and (b) after another 100 cycles at 5*C* rate of the $Li_3V_2(PO_4)_3$/C sample synthesized at 750 °C.

4. Conclusions

The high performance $Li_3V_2(PO_4)_3$/C cathode material with low carbon content is successfully synthesized through a fast sol–gel method based on the spontaneous chemical reactions. This novel method not only possesses the advantage of low energy consumption, but also has a simple synthesis process. The SEM images show that the morphology of the sample exhibits a loose porous microstructure, and a thin carbon layer has been observed on the surface of the $Li_3V_2(PO_4)_3$/C particles through TEM analysis. The charge and discharge tests prove that the sample sintered at 750 °C for 8 h has the best electrochemical performance, delivering the discharge capacities of 127.9 mAh g^{-1} and 124.0 mAh g^{-1} after 100 cycles at 1*C* and 5*C* rates respectively. In addition, the sample sintered at 750 °C also manifests the high rate capability and long term cyclic performances. The optimal $Li_3V_2(PO_4)_3$/C composite still retains the capacities of 117.6 mAh g^{-1}, 114.9 mAh g^{-1} and 83.6 mAh g^{-1} in 150th cycle with the capacity retention of 96.5%, 94.3% and 69.7% at 10*C*, 15*C* and 20*C* rates respectively. We attribute the excellent electrochemical performance of the synthesized material to the coating carbon and the loose porous microstructure. Hence, the novel method in this paper is a promising route to synthesize high performance $Li_3V_2(PO_4)_3$/C cathode material.

Acknowledgements

This work was supported by National Nature Science Foundation of China (Grant No. 20973124) and the Key Project of Guangdong Science and Technology (Grant No. 2009A080208001).

References

[1] R. Yazami, N. Lebrun, M. Bonneau, M. Molteni, High performance $LiCoO_2$ positive electrode material, J. Power Sources 54 (1995) 389–392.
[2] T. Nohma, H. Kurokawa, M. Uehara, M. Takahashi, K. Nishio, T. Saito, Electrochemical characteristics of $LiNiO_2$ and $LiCoO_2$ as a positive material for lithium secondary batteries, J. Power Sources 54 (1995) 522–524.
[3] F. Capitaine, P. Gravereau, C. Delmas, A new variety of $LiMnO_2$ with a layered structure, Solid State Ionics 89 (1996) 197–202.
[4] M.M. Thackeray, Spinel electrodes for lithium batteries, J. Am. Ceram. Soc. 82 (1999) 3347–3354.
[5] J.W. Fergus, Recent developments in cathode materials for lithium ion batteries, J. Power Sources 195 (2010) 939–954.
[6] A.K. Padhi, K.S. Nanjundaswamy, C. Masquelier, J.B. Goodenough, Mapping of transition metal redox energies in phosphates with NASICON structure by lithium intercalation, J. Electrochem. Soc. 144 (1997) 2581–2586.
[7] H. Huang, S.C. Yin, T. Kerr, N. Taylor, L.F. Nazar, Nanostructure composites: a high capacity, fast rate $Li_3V_2(PO_4)_3$/carbon cathode for rechargeable lithium batteries, Adv. Mater. 14 (2002) 1525–1528.
[8] S.C. Yin, H. Grondey, P. Strobel, H. Huang, L.F. Nazar, Charge ordering in lithium vanadium phosphates: electrode materials for lithium-ion batteries, J. Am. Chem. Soc. 125 (2003) 326–327.
[9] S.C. Yin, P.S. Strobel, H. Grondey, L.F. Nazar, $Li_{2.5}V_2(PO_4)_3$: a room-temperature analogue to the fast-ion conducting high-temperature γ-phase of $Li_3V_2(PO_4)_3$, Chem. Mater. 16 (2004) 1456–1465.
[10] A.P. Tang, X.Y. Wang, G.R. Xu, R.H. Peng, H.D. Nie, Chemical diffusion coefficient of lithium ion in $Li_3V_2(PO_4)_3$ cathode material, Mater. Lett. 63 (2009) 2396–2398.
[11] Y.Q. Qiao, X.L. Wang, Y.J. Mai, J.Y. Xiang, D. Zhang, C.D. Gu, J.P. Tu, Synthesis of plate-like $Li_3V_2(PO_4)_3$/C as a cathode material for Li-ion batteries, J. Power Sources 196 (2011) 8706–8709.
[12] X.H. Rui, Y. Jin, X.Y. Feng, L.C. Zhang, C.H. Chen, A comparative study on the low-temperature performance of $LiFePO_4$/C and $Li_3V_2(PO_4)_3$/C cathodes for lithium-ion batteries, J. Power Sources 196 (2011) 2109–2114.
[13] H. Tukamoto, A.R. West, Electronic conductivity of $LiCoO_2$ and its enhancement by magnesium doping, J. Electrochem. Soc. 144 (1997) 3164–3168.
[14] J.W. Wang, J. Liu, G.L. Yang, X.F. Zhang, X.D. Yan, X.M. Pan, R.S. Wang, Electrochemical performance of $Li_3V_2(PO_4)_3$/C cathode material using a novel carbon source, Electrochim. Acta 54 (2009) 6451–6454.
[15] T. Jiang, W.C. Pan, J. Wang, X.F. Bie, F. Du, Y.J. Wei, C.Z. Wang, G. Chen, Carbon coated $Li_3V_2(PO_4)_3$ cathode material prepared by a PVA assisted sol–gel method, Electrochim. Acta 55 (2010) 3864–3869.
[16] X.H. Rui, C. Li, J. Liu, T. Cheng, C.H. Chen, Composites with high-rate capability prepared by a maltose-based sol–gel route, Electrochim. Acta 55 (2010) 6761–6767.
[17] Y.Q. Qiao, X.L. Wan, Y. Zhou, J.Y. Xiang, D. Zhang, S.J. Shi, J.P. Tu, Electrochemical performance of carbon-coated $Li_3V_2(PO_4)_3$ cathode materials derived from polystyrene-based carbon-thermal reduction synthesis, Electrochim. Acta 56 (2010) 510–516.
[18] J. Zhai, M.S. Zhao, D.D. Wang, Y.Q. Qiao, Effect of MgO nanolayer coated on $Li_3V_2(PO_4)_3$/C cathode material for lithium-ion battery, J. Alloys Compd. 502 (2010) 401–406.
[19] M.M. Ren, Z. Zhou, Y.Z. Li, X.P. Gao, J. Yan, Preparation and electrochemical studies of Fe-doped $Li_3V_2(PO_4)_3$ cathode materials for lithium-ion batteries, J. Power Sources 162 (2006) 1357–1362.
[20] J. Barker, R.K.B. Gover, P. Burns, A. Bryan, The effect of Al substitution on the electrochemical insertion properties of the lithium vanadium phosphate $Li_3V_2(PO_4)_3$, J. Electrochem. Soc. 154 (2007) A307–A313.
[21] J.S. Huang, L. Yang, K.Y. Liu, Y.F. Tang, Synthesis and characterization of $Li_3V_{(2-2x/3)}Mg_x(PO_4)_3$/C cathode material for lithium-ion batteries, J. Power Sources 195 (2010) 5013–5018.
[22] S.K. Zhong, L.T. Liu, J.Q. Liu, J. Wang, J.W. Yang, High-rate characteristic of F-substitution $Li_3V_2PO_4$/C cathode materials for Li ion batteries, Solid State Commun. 149 (2009) 1679–1683.
[23] A.Q. Pan, J. Liu, J.G. Zhang, W. Xu, G.Z. Cao, Z.M. Nie, B.W. Arey, S.Q. Liang, Nanostructured $Li_3V_2(PO_4)_3$/carbon composite for high-rate lithium-ion batteries, Electrochem. Commun. 12 (2010) 1674–1677.
[24] P. Fu, Y.M. Zhao, Y.Z. Dong, X.N. An, G.P. Shen, Synthesis of $Li_3V_2(PO_4)_3$ with high performance by optimized solid-state synthesis routine, J. Power Sources 162 (2006) 651–657.
[25] X.J. Zhu, Y.X. Liu, L.M. Geng, L.B. Chen, Synthesis and performance of lithium vanadium phosphate as cathode materials for lithium ion batteries by a sol–gel method, J. Power Sources 184 (2008) 578–582.
[26] G. Yang, H.D. Liu, H.M. Ji, Z.Z. Chen, X.F. Jiang, Temperature-controlled microwave solid-state synthesis of $Li_3V_2(PO_4)_3$/C as cathode materials for lithium batteries, J. Power Sources 195 (2010) 5374–5378.
[27] Y.Q. Qiao, J.P. Tu, J.Y. Xiang, X.L. Wang, Y.J. Mai, D. Zhang, W.L. Liu, Effects of synthetic route on structure and electrochemical performance of $Li_3V_2(PO_4)_3$/C cathode materials, Electrochim. Acta 56 (2011) 4139–4145.
[28] M.M. Ren, Z. Zhou, X.P. Gao, W.X. Peng, J.P. Wei, Core-Shell $Li_3V_2(PO4)3$@C composites as cathode materials for lithium-ion batteries, J. Phys. Chem. C 112 (2008) 5689–5693.
[29] X.L. Wu, L.Y. Jiang, F.F. Cao, Y.G. Guo, L.J. Wan, $LiFePO_4$ nanoparticles embedded in a nanoporous carbon matrix: superior cathode material for electrochemical energy-storage devices, Adv. Mater. 21 (2009) 2710–2714.
[30] A.Q. Pan, D. Choi, J.G. Zhang, S.Q. Liang, G.Z. Cao, Z.M. Nie, B.W. Arey, J. Liu, High-rate cathodes based on $Li_3V_2(PO_4)_3$ nanobelts prepared via surfactant-assisted fabrication, J. Power Sources 196 (2011) 3646–3649.
[31] Y.Q. Qiao, X.L. Wang, J.Y. Xiang, D. Zhang, W.L. Liu, J.P. Tu, Electrochemical performance of $Li_3V_2(PO_4)_3$/C cathode materials using stearic acid as a carbon source, Electrochim. Acta 56 (2011) 2269–2275.
[32] H.D. Liu, P. Gao, J.H. Fang, G. Yang, $Li_3V_2(PO_4)_3$/graphene nanocomposites as cathode material for lithium ion batteries, Chem. Commun. 47 (2011) 9110–9112.
[33] B. Kang, G. Ceder, Battery materials for ultrafast charging and discharging, Nature 458 (2009) 190–193.
[34] Y.N. Ko, H.Y. Koo, J.H. Kim, J.H. Yi, Y.C. Kang, J.-H. Lee, Characteristics of $Li_3V_2(PO_4)_3$/C powders prepared by ultrasonic spray pyrolysis, J. Power Sources 196 (2011) 6682–6687.
[35] Y.Q. Wang, J.L. Wang, J. Yang, Y.N. Nuli, High-rate $LiFePO_4$ electrode material synthesized by a novel route from $FePO_4{\cdot}4H_2O$, Adv. Funct. Mater. 16 (2006) 2135–2140.